Journal Home Page: https://sites.google.com/a/univsul.edu.iq/sjes

Computational Study of Heat Transfer Behavior in Fluid-Solid Fluidized Beds

Sherko Ahmad Flamarz
Sulaimani Polytechnic University (SPU), Air Conditioning and Refrigeration Department

Article Inform

Article History:
Received 13 January 2020
Accepted 16 April 2020
Available online 30 December 2020

Keywords: Fluidization, Multiphase flow, Combined CFD-DEM, Heat transfer.

About the Authors:
Corresponding author:
Sherko Ahmad Flamarz
E-mail: sherko.flamarz@spu.edu.iq

DOI Link: https://doi.org/10.17656/sjes.10132

Abstract

Heat transfer in fluid-solid fluidized beds is investigated using a combined of computational fluid dynamics (CFD) and discrete element method (DEM) approach, incorporated with a thermal model. The approach has taken into account almost all the mechanisms in heat transfer in fluidized beds. A comparison and validation of hydrodynamic and thermal data of fluidized bed obtained using CFD-DEM thermal approach with experimental and numerical results data in the literature is carried out. The simulations results reveal a good thermal steady state during the simulation time for calculating the thermal behaviors of fluidized beds like; the mean particle temperature, bed porosity, heat transfer coefficient and mean particle Reynolds number. The simulations results are showed a good agreement and consistency with the experimental and numerical data in the literatures. Thus, the integration of combined CFD-DEM with the thermal model is a step toward for the prediction, development the heat transfer efficiency in fluid-solid system, and the decrease of energy consumption of the industrial applications .

1. Introduction

Many industrial processes and production units include fluidized beds reactors, so it has become necessary to develop the performance of the fluidization units in terms of combustion processes and the heat transfer process in them. Heat transfer in fluidized (fluid-solid) beds systems is a space rich of practical applications in industrial processes. Typical examples of fluid-solid systems include most food manufacturing processes, safe handling and processing of radioactive waste materials, combustion, drying, freezing etc., where knowledge of temperature fields is very important. To realize the best control and design of such processes, it is necessary to understand the methods and behavior of the heat transfer in fluidized bed reactors. Since the development of computers in early 1980^s, the emergence of computer hardware and software programs gave the solutions of complexes problems in industrials sectors. However, many methods (approaches) are proposed to model the heat transfer in granular

media by using kinetic theory, continuum approaches (CFD), Lagrangian approaches (DEM), and combine the Eulerian approach with Lagrangian approaches (CFD-DEM). Modeling the heat transfer in systems that contain large numbers of particles remains a challenge, especially when fluid-particle interactions are taken into account. It is difficult to investigate experimentally fluid-particle systems, a cause of complexity of the system, and limitations of measurement techniques. This difficulty can be overcome by numerical simulation a technique using the combined CFD-DEM this was developed by Tsuji et al. (Tsuji, Kawaguchi and Tanaka, 1993), this combined is used for the simulation of gas-solid flow. In the CFD-DEM coupling method, the Computational Fluid Dynamics (CFD) is solved by locally-averaged Navier-Stokes equations. The motion of discrete particles is treated by the DEM approach, where the particle-particle and particle-wall collision are solved by Newton's second law of motion. It is noted that the number of researches of heat transfer process in the fluidized beds which are based on combined (CFD-DEM) are still very limited. Previously, the CFD-DEM method is used for modeling the gas-solid fluidized beds coupling for heat transfer. Researchers have been proposed to study the heat transfer in gas-fluidized beds can be found in the literature (Patil, Peters and Kuipers, 2015) (Wang, Zhong, Wang and Alting, 2015) (Zhou, Z., Yu, A. and Zulli, P. 2010). However, the coupling of CFD-DEM has implemented in various areas of research fields and industrial applications. Gan et al. (Gan, Zhou, and Yu, 2016) extended a combined approach of CFD-DEM, to study the heat transfer in packed and fluidized beds. Tal et al. (Tsory, Ben-Jacob, Brosh and Levy, 2013) studied the heat transfer simulations for predicting the effective thermal conductivity (ETC) of particulate beds under compression. Malone, and Xu (Malone, and Xu, 2008) examined the particle-scale flow and heat transfer behavior, Li et al. (Li, Mason, and Mujumdar, 2003) were developed A two-dimensional numerical model to simulate heat transfer in gas-solids flows through pipes, and Kaneko et al. (Kaneko, Shiojima, and Horio, 1999) studied polymerization reactions in gas-fluidized beds and convective heat transfer between particles and the gas. Other authors (Brosh and Levy, 2010) (Brosh, Kalman and Levy, 2010) (Shimizu, 2006) (Al-Arkawazi, Marie and Coorevits, 2018) had proposed models of coupling DEM-CFD, which was used to simulate heat transfer in a pneumatic conveying system, fluidized beds, etc.

2. Aims of the study

The aims of the current paper are developing and implementing particle-wall and fluid-wall convective heat transfer in a combined CFD-DEM thermal approach. Then the thermal approach is used to study and describe the behavior of heat transfer in fluid-solid fluidized beds, predicting the heat transfer coefficient between the solid phase and the fluid phase, and optimize the heat transfer efficiency in fluid-solid (particle) systems for improving and decrease energy consumption of the industrial applications.

3. Numerical model

A combined thermal CFD-DEM model was developed for modeling and simulating heat transfer in fluidized beds. The approach has taken into account almost all the mechanisms in heat transfer, including particle-particle conduction and particle-fluid convection.

In this paper, the following assumptions were made; the particles are spherical and incompressible; physical properties of particle and fluid such a heat capacity, thermal conductivity, density, and young modulus are considered to be constant; there are no chemical interactions; and radiation heating can be neglected at low temperature (less than 400 °C) (Zabrodsky, 1966).

3.1. Governing equations for fluid phase (continuum approach CFD)

The fluid dynamics is a branch of fluid mechanics, which deals with the fluid in motion. The basic governing equations of fluid motion are called the Navier-Stokes equations, which govern the motion of a viscous, non-viscous, compressible and incompressible fluid flows. In the present study, numerical software Code Saturne (version 4) is used (Archambeau, Méchitoua and Sakiz, 2004). Code Saturne is generalist Computational Fluid Dynamics (CFD) produced by Electricity De France (EDF). The fluid flow fields are calculated from the conservation equations; mass (continuity) and momentum (Navier–Stokes equations) for an incompressible fluid (Launder, B. E. and Spalding, 1974), which can be expressed by;

Continuity equation (mass balance):

$$\frac{\partial \rho_f}{\partial t} + \vec{\nabla}.\left(\rho \vec{u}_f\right) = 0 \qquad (1)$$

Momentum equation of the quantity of motion:

$$\frac{\partial \rho_f \ \vec{u}_f}{\partial t} + \vec{\nabla}.\left(\vec{u}_f \otimes \vec{u}_f\right) = -\vec{\nabla}p + \vec{\nabla}.\bar{\bar{\tau}} + \rho_f \vec{f} \qquad (2)$$

Shear stress constitutive equation:

$$\bar{\bar{\tau}} = -\mu\left(\nabla \vec{u}_f + \nabla \vec{u}_f f^T - \frac{2}{3}\nabla \vec{u}_f\right) \qquad (3)$$

Where t is time, ρ_f , $\vec{u}_f$ and p are density, velocity, and pressure of the fluid respectively, $\bar{\bar{\tau}}$ is the viscous stress tensor and $\vec{f}$ refers to other body forces. In general most CFD codes are required software for geometry design, meshing and visualization, so the platform as Salome (version 8) has been used in this work, which provides a generic platform for Pre-Processing and Post-Processing for numerical simulation. The assumptions were no-slip boundaries and unstructured meshes are used for the column walls in the CFD model. The k-ε model is used in this work, which largely applied for its simplicity (Launder, B. E. and Spalding, 1974).

3.2. Governing equations for solid phase (discrete approach DEM)

The Lagrangian approach or Discrete Element Method (DEM) are developed by Cundall and Strack (Cundall and Strack, 1979), which they used the discrete model for study the soil mechanic. The DEM model, the trajectories and rotations of individual particles are evaluated based on Newton's second law of motion, using a numerical time stepping scheme where contact forces are calculated at each time step using appropriate contact laws. So, the motion of the i th particle is governed by the laws of linear momentum conservation and angular momentum (Cundall and Strack, 1979), expressed by:

$$m_{p,i}\frac{d\vec{u}_{p,i}}{dt} = \vec{F}_{D,p,i} + m_{p,i}\vec{g} + \sum_{j=1}^{nc}\vec{F}_{C,ij} \qquad (4)$$

$$\vec{F}_{C,i} = \vec{F}_{t,i}.t + \vec{F}_{n,i}.n \qquad (5)$$

$$I_{p,i}\frac{d\vec{\omega}_{p,i}}{dt} = \sum_{j=1}^{nc}\left(\vec{T}_{t,ij} + \vec{T}_{f,ij}\right) \text{ and } I_{p,i} = \frac{2}{5}m_{p,i}r_{p,i}^2 \qquad (6)$$

where $m_{p,i}$, $r_{p,i}$ $u_{p,i}$ and $\vec{\omega}_{p,i}$ represent the mass, radius, the translational and angular velocities of the i th particle, respectively. $\vec{F}_{D,p,i}$ is the fluid-particle interaction force (drag force), $m_{p,i}$ g the gravitational force, nc is the number of contacts between the particles and the particle i, and $\vec{F}_{C,ij}$ is the inter-particle forces between particles which include contact force ($\vec{F}_{n,i}$ normal and $\vec{F}_{t,i}$ tangential) (see Figure 1). $I_{p,i}$ is the moment of inertia of the particle. The torque acting on particle i by particle j includes $\vec{T}_{t.ij}$ generated by tangential force and $\vec{T}_{f.ij}$ is the rolling friction torque. The DEM model has been used to simulate the heat transfer between particle-particle, fluid-particle, and particles-wall. The DEM model has

been used to simulate the heat transfer between particle-particle, fluid-particle, and particles-wall.

3.3. Hydrodynamic interaction fluid-solid systems

Fluid-solid interaction force (exchange the momentum between the fluid and the solid phase), or drag force is determined for each particle. The drag force is modeled and expressed by considering these factors as follows (Helland, Occelli and Tadrist, 2002):

$$F_{D,p,i} = \frac{C_{D,p,i}}{8}\pi\rho_f d_{p,i}^2 \|u_f - u_{p,i}\|(u_f - u_{p,i})\varepsilon_f^2 f(\varepsilon_f)^m \text{ and } f(\varepsilon_f)^m = \varepsilon f^{-m.n} \quad (7)$$

where $C_{D,p,i}$ is the drag coefficient, $d_{p,i}$ is the particle diameter, ρ_f ,u_f ,ε_f are the density, velocity, local porosity of the fluid respectively, and $m.n$ is a parameter, in this study ($m.n$=4,75) (Al-Arkawazi, Marie and Coorevits, 2018). The drag coefficient $C_{D,p,i}$ on a single sphere is a function of Reynolds number of the particle ($Re_{p,i}$), and $C_{D,p,i}$ is given by correlation of Brown and Lawler (Brown and Lawler, 2003):

$$C_{D,p,i} = \frac{24}{Re_{p,i}}\left(1 + 0.15Re_{p,i}^{0.681}\right) + \frac{0.407}{1+\frac{8710}{Re_{p,i}}} \text{ and } Re_{p,i} = \frac{\varepsilon_f d_{p,i}\|u_f - u_{p,i}\|}{\nu_f} \quad (8)$$

Where ν_f is the kinematic viscosity of the fluid, and the local porosity ε_f is calculated by Representative Elementary Volume (REV) method is centered on the particle (Al-Arkawazi, Marie, Benhabib and Coorevits, 2017).

4. Thermal model

When two solid particles of different temperatures approach each other, they begin to exchange heat (thermal energy) due to conduction, convection, and radiation. There are a number of extra parameters associated with the heat transfer process, which depends on the thermal properties of the particles (specific heat and thermal conductivity), particle characteristics (density and particle size). The thermal properties of the fluid must be sufficiently low that the heat transfer coefficient will be significant in thermal processing, the flow rate of the fluid, and the temperature difference between the particles and the fluid (Vargas-Escobar, 2002). In the current work, the mechanisms of heat transfers are introduced in the thermal model (CFD-DEM thermal approach).

Thus the energy balance is:

$$mC_p\frac{dT}{dt} = \Phi_{Cond.} + \Phi_{Conv.} \quad (9)$$

Where;

- $\Phi_{Cond.}$ is the thermal contact conductance between two particles (O_i and O_j), (see **Figure 1**):
  $\Phi_{Cond.}^{ij} = H_C^{ij}(T_j - T_i)$ and $H_C^{ij} = 2\lambda_s a = 2\lambda_s\left(\frac{3F_n a^*}{4E^*}\right)^{\frac{1}{3}}$ (10)

- H_C^{ij} contact conductance between particles O_i and O_j , λ_p is the thermal conductivity of the particle, a is Hertzian contact radius, and a^* is the equivalent radius $\frac{1}{a^*} = \frac{1}{r_i} + \frac{1}{r_j}$, E^* expresses an equivalent Young's modulus between the particles in contact $\frac{1}{E^*} = \frac{\left(1-\nu_i^2\right)}{E_i} + \frac{\left(1-\nu_j^2\right)}{E_j}$, and ν is Poisson's ratio.
- $\Phi_{Conv.}$ is the heat flux transition by convection, express by Newton's law:
  $\Phi_{Conv.} = hS(T_s - T_\infty)$ (11)

where h is the convective heat transfer coefficient between the fluid and particles/walls, S surface area of a contact solid/fluid, T_s temperature of the solid surface, and T_∞ temperature of fluid far away from the solid surface. Many of authors proposed empirical correlations to estimate the value of convective heat transfer coefficient from the calculation of the Nusselt number (Nu) of particles (Ranz and Marshall, 1952) (Li and Mason, 1998) (Kemp, Bahu and Pasley, 1994), and walls (Laguerre, Amara and Flick, 2006). One of the most frequently quoted expressions is that of Ranz and Marshall, to apply the Ranz-Marshall equation to a system of several particles, one needs to know the porosity function connecting the Nusselt number for a particle in a fluidized system, with that of a particle isolated at the same superficial fluid velocity (Li and Mason, 2000). In this paper the value of heat transfer coefficient between the fluid and the particles is calculated from the correlation of Gunn;

$$Nu_{p,i} = \left(7 - 10\varepsilon_f + 5\varepsilon_f^2\right)\left(1 + 0.7Re_{p,i}^{0.2}Pr^{0.33}\right) + \left(1.33 - 2.4\varepsilon_f + 1.2\varepsilon_f^2\right)Re_{p,i}^{0.7}Pr^{0.33} \quad (12)$$

where the Nusselt number of the particle ($Nu_{p,i} = \frac{h_i . d_{p,i}}{\lambda_f}$), Prandtl number ($Pr = \frac{C_f \cdot \mu_f}{\lambda_f}$), and for heat transfer coefficient between the fluid and the wall (Laguerre, Amara and Flick, 2006); ($Nu_w = 1.56\, Re_D^{0.53}\, Pr^{0.33}$), ($Re_D = \frac{\rho_f u_f D}{\mu_f}$) and ($Nu_w = \frac{h_w D}{\lambda_f}$), where C_f is the thermal capacity of the fluid, D is the diameter of the column (pipe) and h_w is the wall heat transfer coefficient. Thus, the energy balances of a particle O_i which in contact with (α) particles O_j is given by the following expression:

$$mC_{Pi}\frac{dT_i}{dt} = \sum_{j=1}^{\alpha}\left[H\left(T_j - T_i\right) + \Phi_\mu^{ij} + \Phi_{Impact}^{ij}\right] + \Phi_{Conv.}^{i} \quad (13)$$

Equation 13 was integrated into the DEM model for calculating the temperature of the particle O_i at time ($t+\Delta t$) as follows:

$$T_i^{t+\Delta t} = T_i^t + \frac{\Delta t}{mC_{Pi}}\left[\sum_{j=1}^{\alpha}\left[H_C^{ij}\left(T_j^t - T_i^t\right)\right] + \Phi_{Conv.}^{i}\right] \quad (14)$$

The other part of the thermal model for the heat transfer between the particle and the fluid is done by using a model of conduction-convection based on the finite volume method. The system is divided into rectangular elements which may contain a plurality of particles or parts of particles.

$$m_{i,j}^f C_{Pi}^f\left(\frac{T_{i,j}^{f,t+\Delta t} - T_{i,j}^{f,t}}{\Delta t} + U_x^f\frac{T_{i+1,j}^{f,t} - T_{i-1,j}^{f,t}}{2\Delta x} + U_y^f\frac{T_{i,j+1}^{f,t} - T_{i,j-1}^{f,t}}{2\Delta y}\right) = \lambda^f S^f\left(\frac{T_{i+1,j}^{f,t} - T_{i,j}^{f,t} + T_{i-1,j}^{f,t}}{\Delta x^2} + \frac{T_{i,j+1}^{f,t} - T_{i,j}^{f,t} + T_{i,j-1}^{f,t}}{\Delta y^2}\right) + \sum_{i=1}^{\gamma} h_p^f S_p^f\left(T_k^t - T_{i,j}^{f,t}\right) \quad (15)$$

where $m_{i,j}^f$, C_{Pi}^f and λ^f are respectively the fluid mass contained in the element, the heat capacity and the thermal conductivity of the fluid, S_p^f represent the particle surface in contact with the fluid in the element, T_k is the temperature of the particles, $T_{i,j}^f$ the temperature of fluid is considered constant in each element. Note that $T_{i,0}^{f,t}$ is the fluid temperature at the inlet of the model. At the exit, we consider $T_{i,n}^{f,t}$ is equal to $T_{i,n-1}^{f,t}$. Thus, the computational tasks at each time step (Δt) can be summarized as: (*i*) detect the contact between particles, thus updating neighbor lists, (*ii*) compute contact forces, (*iii*) compute drag force on the particle, (*iv*) compute the heat fluxes using thermal properties, (*v*) sum all forces and heat fluxes on particles and update particle position and temperatures, and (*vi*) determine the trajectory of the particle using Newton's laws of motion.

5. Results and discussions

The numerical simulations are becoming a strong tool that helps to illustrate the precision of coupling implementation efficiency for heat transfer problems.

5.1. Validation with experimental results

In this part, validation has been done with a thermal (heating and cooling) problem granular material (fluidized beds), studied experimentally and numerically (heating and cooling) by Ehsani et al. (Ehsani, Movahedirad and Shahhosseini, 2016). A fluidized bed column with diameter (D = 8 cm) and height (H= 60 cm) is used. The bed is composed of steel spheres (height of the bed at rest h = 27 cm), and the thickness of the bed is equal to one particle diameter (d_p =3 mm), in order to reduce the number of particles in the simulation. The fluid (water) properties are assumed to be constant all throughout the simulations, and the material parameters are detailed in **Table 1**. The initial temperature of the particles were 25°C, which heated by hot water flows upwardly through the granular with inlet temperature 100°C through the bed. The particles are fluidized and heated along the direction of flow for 15 seconds (simulation time). Then subsequently, after switching off the hot water, the cold water enters the column with inlet temperature 25°C for 15 seconds. For the two periods of heating and cooling the water has a constant inlet velocity (u_f = 0.187 m/s). The outlet temperature of the water (T_o) is normalized, as expressed;

$$T_{o,Norm} = \frac{T_o - T_{o,min}}{T_{o,max} - T_{o,min}} \qquad (16)$$

where $T_{o,Norm.}$ normalized outlet water temperature, $T_{o,min.}$ and $T_{o,max.}$ are the minimum and maximum water outlet temperatures in heating or cooling period, respectively. Figure 2, a and b for heating and cooling periods, respectively shows the development of the fluid outlet temperature along the bed for heating and cooling periods as a function of flow time. Figure 2 reveals that the results of the proposed thermal approach in this work are nearest to the experimental results than the simulations results of Ehsani et al. (Ehsani, Movahedirad and Shahhosseini, 2016). This can explain due to our thermal model is based on the finite volume method integrated into CFD-DEM (E-L) model, whilst the Ehsani model is based on (E-E) model. It is known that the multiphase (fluid-solid) flow modeled by E-L model has an advantage on the E-E model. The Eulerian models (E-E) take into account all phases (fluid phase and solid phase) to be continuous and interpenetrating, and the equations employed are a generalization of the Navier-Stocks equations. On the another hand, DEM models solve the Newtonian equations of motion for each individual particle, the effect of collisions forces between particle-particle, and forces acting on the particle by the fluid like the drag force. Thus, the interactions between the fluid and particles are treated more efficient in terms of heat exchange between the particles, and fluid-particles in the fluidized beds. To present the heating/cooling heat transfer (exchange) between the fluid and the particles or vice versa, Figures 3 and 4 show the particle's positions and temperature profile of the fluid (water) in the column over time. The snapshots of Figures 3 and 4, state of the system during the simulation of heat transfer for two cases (heating and cooling) in the fluidization process. Initially, the bed is static (Figures 3 and 4 at t = 0), where velocities of particles are zero, and the changing in the water temperature (heating or cooling) is presented in the second plot. The water inter the column uniformly in an upward direction, passing through the interstitial distance between the particles, producing the interaction fluid-particles force (drag force) excite the particles to fluidize. The snapshots in Figures 3 and 4 (0-2.0 s) are depicted that the bed trends to stability when the forces, such as the fluid-particle interaction force, the contact forces and the buoyancy forces acting on individual particles are balanced. The rate of heat transfer from the fluid

to the particles and vice versa is accelerating with the progress of the fluidization process (2.0-10s). (Note: the temperature profile in Figures 3 and 4 is in Kelvin)

5.2. Heat transfer coefficient

The calculated values of the convective heat transfer coefficient are plotted as a function of bed voidage (porosity) in Figure 5, which depicted that; the value of the heat transfer coefficient is directly proportional to the value of porosity obtained by using Equation 12. The results were averaged over the steady-state simulation for fluidized velocities (0.08, 0.12 and 0.16 m/s) revealed that, the maximum values of heat transfer coefficient at a bed porosity of (ε =0.75, h_i=2300 W/m^2.K), (ε =0.85, h_i=4200 W/m^2.K), and (ε =0.92, h_i =6092 W/m^2.K) respectively (see Figure 5). Hence, the increase of inlet fluid velocity makes the particles to dispersed in the fluid, this process increase the bed voidage (porosity) of the fluidized bed and develop the convective heat transfer coefficient, this leads to the enhancement of heat exchange between particles and fluid by convection. Figure 6 shows an increase in the convective heat transfer coefficient value with the value of the mean particle Reynolds number. Thus the high velocity of fluidization is forced the particles to good mixing, moving and heat energy to exchange between the particles, and with fluid in the fluidized space. It should be aware to the nature of the industrial application, to identify and diagnose the fluid velocity and temperature to be applied.

6.Conclusions

In this study, a thermal approach has been developed to take into account the convective heat transfer between the fluid and the particles, and the wall of the column. Comparison and validation of thermal data for the thermal approach with experimental and numerical results data in the literature are carried out. The results showed that thermal approach was well integrated with the combined CFD- DEM model and has proven its effectiveness for fluid-solid fluidized bed. The simulations results show that the reveals a good thermal steady state during the simulation time for calculating the thermal behaviors for fluidized beds like the mean particle temperature, bed voidage (porosity), convective heat transfer coefficient and mean particle Reynolds number. The simulations results showed that; the increase of the heat transfer coefficient value with the value of bed porosity or mean particle Reynolds number is not necessarily enhance the heat transfer to or from the particle. This returns to the physical properties of the particles and the fluid, because it needs to provide sufficient time for the exchange of the heat transfer process.

References

1- Tsuji, Y., Kawaguchi, T. and Tanaka, T. 'Discrete particle simulation of two-dimensional fluidized bed,' Powder Technology, vol.77: pp.79–87, 1993.
2- Patil, A.V., Peters, E.A.J.F. and Kuipers, J.A.M. 'Comparison of CFD-DEM heat transfer simulations with infrared/visual measurements', Chemical Engineering Journal, vol. 277, 1, pp. 388-401, 2015.
3- Wang, C., Zhong, Z., Wang, X. and Alting, S. A. 'Numerical simulation of gas-solid heat transfer behavior in rectangular spouted bed,' Canadian Journal of Chemical Engineering, 93, pp. 2077-2083, 2015.
4- Zhou, Z., Yu, A. and Zulli, P. 'A new computational method for studying heat transfer in fluid bed reactors,' Powder Technology, vol.197, pp. 102-110, 2010.
5- Gan, J., Zhou, Z. and Yu, A. 'Particle scale study of heat transfer in packed and fluidized beds of ellipsoidal particles,' Chemical Engineering Science, vol. 144, pp. 201-215, 2016.
6- Tsory, T., Ben-Jacob, N., Brosh, T. and Levy, A. 'Thermal DEM–CFD modeling and simulation of heat transfer through packed bed,' Powder Technology, vol. 244, pp. 52-60, 2013.
7- Malone, F. and Xu, B.H. 'Particle-scale simulation of heat transfer in liquid-fluidized beds,' Powder Technology, vol. 184, pp. 189-204, 2008.
8- Li, J.T., Mason, D.J. and Mujumdar, A.S. 'A numerical study of heat transfer mechanisms in gas–solids flows through pipes using a coupled CFD and DEM model,' Drying Technology, vol. 21, pp. 1839-1866, 2003.
9- Kaneko, Y., Shiojima, T. and Horio, M. 'DEM simulation of fluidized beds for gas-phase olefin polymerization,' Chemical Engineering Science, vol. 54, pp. 5809-5821, 1999.

10- Brosh, T. and Levy, A. 'Modeling of heat transfer in pneumatic conveyer using a combined DEM–CFD numerical code,' Drying Technology, vol. 28, pp.155-164, 2010.
11. Brosh, T., Kalman, H. and Levy, A. 'DEM simulation of particle attrition in dilute-phase pneumatic conveying,' Granular Matter, vol. 2, pp.175-181, 2010.
12. Shimizu, Y. 'Three-dimensional simulation using fixed coarse-grid thermal-fluid scheme and conduction heat transfer scheme in distinct element method,' Powder Technology, vol. 165, pp. 140-152, 2006.
13. Al-Arkawazi, S., Marie, C. and Coorevits, P.'Modeling the heat transfer between fluid-granular medium,' Applied Thermal Engineering, vol. 128, pp. 696–705, 2018.
14. Archambeau, F., Méchitoua, N. and Sakiz, M. ' Code saturne : A finite volume code for the computation of turbulent incompressible flows - industrial applications,' International Journal on Finite Volumes, vol. 1, no.1, pp. 1-62, 2004.
15. Zabrodsky, S.S. 'Hydrodynamics and Heat Transfer in Fluidized Beds,' M.I.T Press, Cambridge, Massachusetts, 1966.
16. Launder, B. E. and Spalding, D. B. 'The numerical computation of turbulent flows,' Computer Methods in Applied Mechanics and Engineering, vol. 3, 2, pp. 269-289, 1974 .
17. Cundall, P.A. and Strack, O.D.L. 'A discrete numerical model for granular assemblies,' Geotechnique 29 (1979) 47.
18. Helland, E., Occelli, R. and Tadrist, L. 'Computational study of fluctuating motions and cluster structures in gas-particle flows,' International Journal of Multiphase Flow, vol. 28,pp. 199-223, 2002.
19. Brown, P. and Lawler, D. 'Sphere drag and settling velocity revisited,' Journal Environment Engineering, 129, 3, pp. 222–231, 2003.
20. Al-Arkawazi, S., Marie, C., Benhabib, K. and Coorevits, P.'Modeling the hydrodynamic forces between fluid–granular medium by coupling DEM-CFD,' Chemical Engineering Research and Design, vol. 117, pp. 439–447, 2017.
21. Vargas-Escobar, W.L.'Discrete Modeling of Heat Conduction in Granular Media,' University of Pittburgh, Ph.D. thesis, 2002.
22. Ranz, W. E. and Marshall, W. R. 'Evaporation from drops : 1,' Chemical Engineering Progress, Vol. 48, pp. 141, 1952.
23. Li, J. and Mason, D. 'Simulation of gas-solids flow in pipes with heat transfer using the distinct element method,' Chem E Research Event, paper 71, published by Institution of Chemical Engineers, Rugby, UK, 1998.
24. Kemp, I. C., Bahu, R. E. and Pasley, H. S. 'Model development and experimental studies of vertical pneumatic conveying dryers,' Drying Technology, vol. 12, pp.1323–1340, 1994.
25. Laguerre, O., Amara, S. B. and Flick, D. 'Heat transfer between wall and packed bed crossed by low velocity air flow,' Applied Thermal Engineering, vol. 26, pp.1951–1960, 2006.
26. Li, J. and Mason, D. 'A computational investigation of transient heat transfer in pneumatic transport of granular particles,' Powder Technology, vol. 112, pp. 273–282, 2000.
27. Ehsani, M., Movahedirad, S. and Shahhosseini, S.'The effect of particle properties on the heat transfer characteristics of a liquid-solid fluidized bed heat exchanger,' International Journal of Thermal Sciences vol.102, pp.111-121, 2016.

دراسة حسابية لسلوك انتقال الحرارة بين المائع- الصلب في الطبقة المميعة

أ.م.د. شيركو احمد فلامرز

جامعة السليمانية التقنية، قسم التكييف والتبريد

المستخلص

يتم دراسة انتقال الحرارة في الطبقة المميعة ذات المائع- الصلب عن طريق الجمع بين طريقة ديناميات الموائع الحسابية (CFD) وطريقة العناصر المنفصلة (DEM) ، مدمجة مع نموذج حراري. لقد أخذت المقاربة في الحسبان معظم آليات انتقال الحرارة في الطبقة المميعة. تم إجراء المقارنة والتحقق من صحة البيانات الهيدروديناميكية والحرارية للطبقة المميعة التي تم الحصول عليها باستخدام مقاربة CFD-DEM الحراري مع بيانات النتائج التجريبية والعددية في البحوث المنشورة سابقا. اظهرت نتائج المحاكاة عن حالة استقرار وثبوت حراري جيد خلال وقت المحاكاة لحساب السلوكيات الحرارية للطبقة المميعة مثل ؛ متوسط درجة حرارة الجسيمات ، مسامية الطبقة المميعة ، معامل انتقال الحرارة و متوسط عدد رينولدز للجسيمات. وأظهرت نتائج المحاكاة اتفاق واتساق جيد مع البيانات التجريبية والعددية مع البحوث المنشورة سابقا. اذا فإن جمع CFD-DEM المدمج مع النموذج الحراري هو خطوة نحو التنبؤ وتطوير كفاءة انتقال الحرارة في نظام المائع- الصلب وتقليل استهلاك الطاقة للتطبيقات الصناعية.

الكلمات المفتاحية: التميع ، التدفق متعدد المراحل ، دمج CFD-DEM ، انتقال الحرارة.

Nomenclatures

m	mass of particle [kg]
r, a	radius of particle [m]
d	diameter of particle [m]
D	diameter of column (pipe)[m]
S	surface area of the particle [m^2]
g	acceleration due to gravity [m/s^2]
t	time [s]
u, v	velocity [m/s]
p	pressure of fluid [N/m^2], [Pa]
T	Temperature [°C], [K]
C	thermal capacity [J/°C], [J/K]
f	other body force [N]
F_D	drag force [N]
F_C	contact force [N]
nc	number of contacts [-]
F_t	tangential (frictional) force [N]
F_n	normal force [N]
C_D	drag force coefficient [-]
n	normal unit vector [-]
I	moment of inertia [$(kg \cdot m^2)/rad^2$]
T_t	tangential torque [N.m]
T_f	rolling torque [N.m]
h	heat transfer coefficient [$W/(m^2.K)$]
E^*	equivalent young's modulus, [GPa]

Greek letters

ρ	density [kg/m^3]
μ	viscosity [Pa.s]
ν	kinematic viscosity [m^2/s]
v	Poisson's ratio [-]
τ	viscous stress tensor [N/m^2, Pa]
ω	angular velocity [rad/s]
ε	porosity (void fraction) [-]
λ	thermal conductivity [W/(m.°C)], [W/(m.K)]
Φ	heat transfer energy [(N.m)/s], [J/s], [W]

Dimensionless numbers

Re	Reynolds number
Nu	Nusselt number
Pr	Prandtl number

Subscripts

f	fluid phase
p	particle (solid) phase
i	for i-th particles (solid phase)
i,j	between particle i and particle j

Table 1: Physical properties and dimensions of simulated system.

Particle properties (Aluminum)		Fluid properties (Water)	
Particle diameter, d_p	1.5 mm	Viscosity, μ_f	0.001 kg/m.s
Density, ρ_p	2700 kg/m^3	Density, ρ_f	1000 kg/m^3
Heat capacity, C_p	900 J/kg.K	Heat capacity, C_f	4200 J/kg.K
Thermal conductivity, λ_p	237 W/m.K	Thermal conductivity, λ_f	0.6 W/m.K
Number of particles	2244	Bed height	75 cm
Young modulus	69 GPa	Bed width	5.1 cm
Poisson ratio	0.35	Bed thickness	0.15 cm
Friction coefficient, μ	0.4	Time step, Δt	$5x10^{-6}$ sec

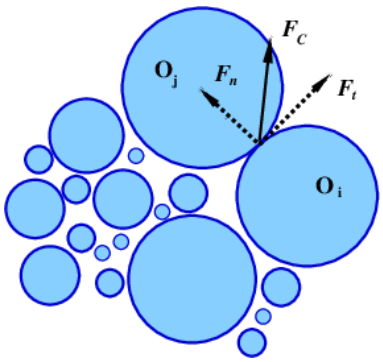

Fig.1: Discrete medium.

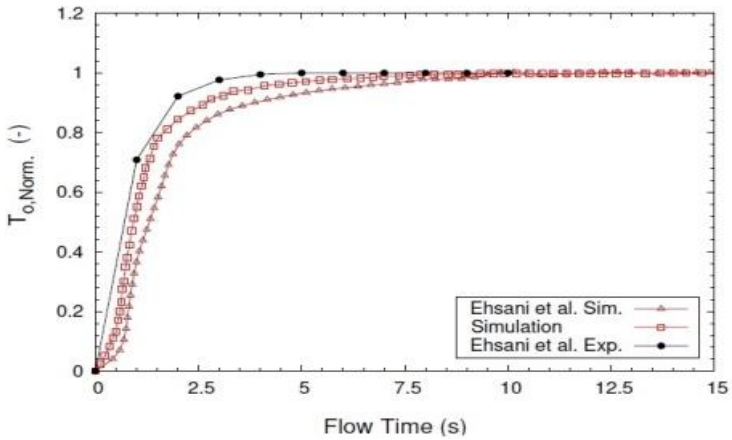

(a)

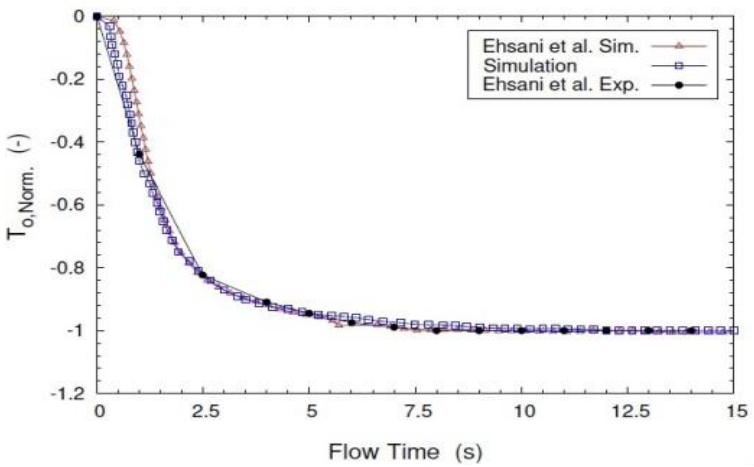

(b)

Fig. 2: Normalized outlet fluid temperature as a function of flow time for,
(a) heating
(b) cooling periods with u_f= 0.187 (m/s).

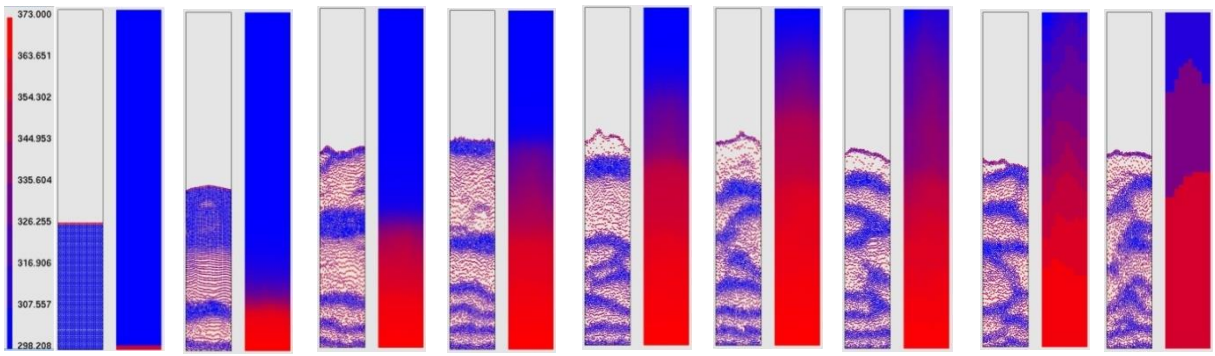

a) t = 0.0 s b)t=0.4s c) t= 0.8s d) t=1.2 s e) t=1.6 s f) t=2.0s g) t= 6.0s h) t=8.0s i) t= 10 s

Fig. 3: Snapshots of the heating period for fluidized bed with fluid velocity u_f = 0.187 m/s.

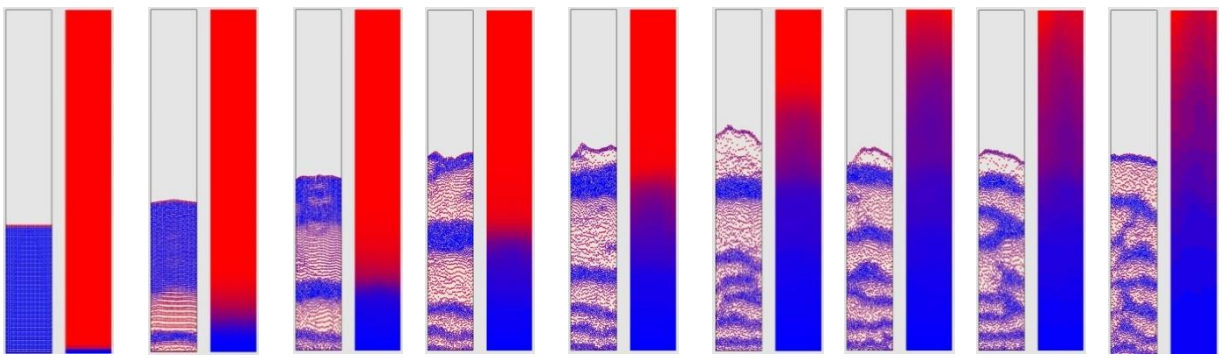

a) t = 0.0 s b) t= 0.25s c) t=0.8 s d) t=0.75s e) t=1.6 s f) t =2.0s g) t =6.0s i) t=8.0s j) t =10s

Fig. 4: Snapshots of the cooling period for fluidized bed with fluid velocity u_f = 0.187 m/s.

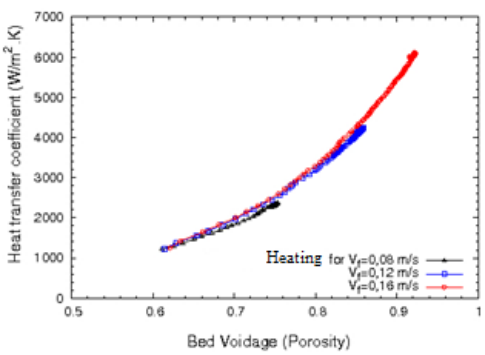

Fig. 5: Heat transfer coefficient as a function of bed voidage (porosity) for Timpose = 100 °C.

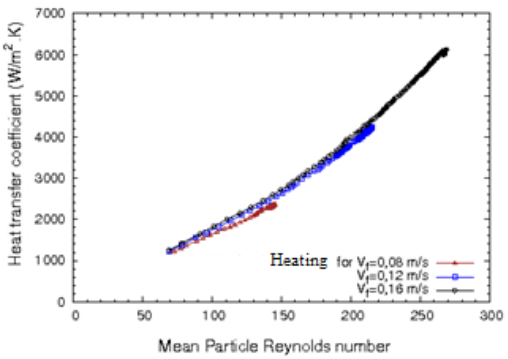

Fig. 6: Heat transfer coefficient as a function of Mean particle Reynolds number for Timpose = 100 °C.